Nature of the smectic-A–hexatic-B–crystal-B transitions of a liquid-crystal compound

A. J. Jin,[1] M. Veum,[1] T. Stoebe,[2] C. F. Chou,[3] J. T. Ho,[3] S. W. Hui,[4] V. Surendranath,[5] and C. C. Huang[1,*]

[1]*School of Physics and Astronomy, University of Minnesota, Minneapolis, Minnesota 55455*

[2]*Department of Chemical Engineering and Materials Science, University of Minnesota, Minneapolis, Minnesota 55455*

[3]*Department of Physics, State University of New York at Buffalo, Buffalo, New York 14260*

[4]*Department of Biophysics, Roswell Park Cancer Institute, Buffalo, New York 14263*

[5]*Department of Physics, Kent State University, Kent, Ohio 44242*

(Received 29 June 1995)

High-resolution heat-capacity, optical reflectivity, and electron-diffraction measurements have been conducted on thin free-standing films of a liquid-crystal compound exhibiting the smectic-A–hexatic-B–crystal-B transitions. Despite the absence of herringbone order, the liquid-hexatic transition in extremely thin films has been found to show a pronounced pretransitional heat-capacity anomaly, in disagreement with the predictions of two-dimensional melting theory. In addition, both the surface-enhanced layer-by-layer transition near the smectic-A–hexatic-B and an unexpected layer thinning transition above the bulk isotropic-smectic-A transition temperature have been observed.

PACS number(s): 64.70.Md, 61.30.Eb

I. INTRODUCTION

The advance of the theory of defect-mediated phase transitions in two-dimensional XY systems by Kosterlitz and Thouless [1] has generated immense interest and an extensive research effort concerning the subject. Their original ideas were later extended by Halperin and Nelson [2], and Young [3] to describe a process by which a two-dimensional solid could melt, via two Kosterlitz-Thouless (KT)- type transitions, through an intermediate hexatic phase into the isotropic phase. The hexatic phase in two dimensions is characterized by the existence of quasi-long-range bond-orientational order with short-range translational order. According to the theory, both the isotropic-hexatic and hexatic-solid transitions can be represented by two-component order parameters. For example, the order parameter associated with the former can be written as $\Psi=\Psi_0 e^{6i\theta}$ and so the transition should belong to the XY universality class.

Numerous experimental efforts have been undertaken to test these exciting theoretical predictions [4]. So far, the concept of the hexatic order has been found to be extremely helpful in describing several phenomena found in condensed matter [4]. Major conclusions about the existence of the hexatic order can be drawn from structural information, namely, the spatial variation of the positional and bond-orientational correlation function. With the exception of liquid crystals, for most physical systems it is extremely difficult, if not impossible, to characterize the nature of the liquid-hexatic and/or hexatic-solid transitions. Consequently, studies of several liquid-crystal systems have proven to be among the most fruitful.

A pioneering x-ray study of the liquid-crystal compound 65OBC provided the first indication of the existence of a mesophase possessing the three-dimensional long-range bond-orientational order without translational order [5]. This compound is a member of the *n-alkyl*-4′-*n-alk*oxybiphenyl-4-carboxylate (*nm*OBC) homologous series with the following molecular structure:

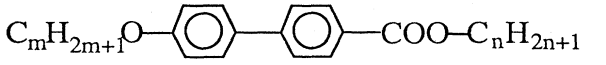

In this phase of 65OBC, the x-ray work also revealed the existence of herringbone order, but a detailed investigation to determine the range of the herringbone order was not performed. Despite the indication of herringbone order, this phase is simply denoted as the hexatic-B (Hex-B) phase and is generally thought of as a stack of two-dimensional hexatic molecular layers resulting in three-dimensional long-range hexatic order. Upon increasing temperature, the compound in this phase melts (through a continuous transition) into the smectic-A (Sm-A) phase, a stack of two-dimensional liquid layers. Upon cooling, the compound transforms (through a first-order transition) into the orthorhombic crystal-E (Cry-E) phase, which exhibits long-range translational and herringbone orientational order.

In light of the unusual behavior near the Sm-A–Hex-B transition of many bulk *nm*OBC samples [4], our research group has constructed a state-of-the-art calorimetric system [6,7] to investigate physical properties of two-layer free-standing liquid-crystal films. Simultaneous measurements of heat capacity and optical reflectivity from two-layer 3(10)OBC films revealed a divergent heat-capacity anomaly [8] near the continuous Sm-A–Hex-B transition. The sharp heat-capacity peak at the transition temperature T_c can be well characterized by a conventional power-law expression

$$C_p = A\,|t|^{-\alpha} + B + Dt\ , \tag{1}$$

with the critical exponent $\alpha=0.31\pm0.03$ [9]. Here the reduced temperature $t=(T-T_c)/T_c$. These experimental results strongly disagree with the theoretical predic-

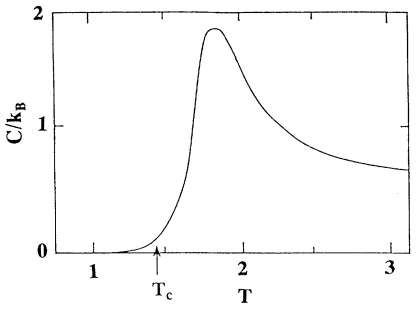

FIG. 1. Vortex contribution to the heat capacity in the 2D *XY* model. T_c ($=T_{KT}$) is the Kosterlitz-Thouless transition temperature.

tion for two-dimensional melting [10,11]. It is instead predicted that the heat capacity should involve only an essential singularity at T_c, which is not expected to be observable, as well as a broad hump above T_c due to the gradual dissociation of defect pairs (see Fig. 1).

Monte Carlo simulations based on a coupled *XY* model proposed by Bruinsma and Aeppli [12] describing the simultaneous creation of both hexatic and herringbone molecular orders yield a single heat-capacity anomaly with $\alpha=0.36\pm0.05$ [13] in appropriate parameter spaces. Subsequently, overexposed electron-diffraction studies on an eight-layer 3(10)OBC film revealed weak herringbone order in the Hex-*B* phase [see Fig. 2(a)]. Thus the discrepancy between the experimental results and theoretical prediction may be argued to be primarily due to the presence of herringbone orientational order in these compounds. Further diffraction studies on herringbone order in the Hex-*B* phase of *nm*OBC samples are essential to clarify the role of this additional molecular order through the Sm-*A*–Hex-*B* transition. Regardless of the scattering results, it is an important experimental task to identify and characterize compounds exhibiting the liquid-hexatic-crystal transition sequence in the absence of herringbone order and to investigate the structural and thermal properties of thin films.

The paucity of liquid-crystal compounds that exhibit the Hex-*B* phase has meant that virtually every investigation of the nature of this intriguing phase and related phase transitions has utilized one of the *nm*OBC compounds. Studies of several other compounds exhibiting the Sm-*A*–Hex-*B*–Cry-*B* sequence have been limited to bulk samples [14,15] or thick films [16]. Employing optical microscopy and low-resolution x-ray studies, Surendranath *et al.* [17] have identified the Hex-*B* phase in some members of the *n*4COOBC (*n-alkyl*-4′-*n*-pentanoyloxy-biphenyl-4-carboxylate) homologs. The molecular structure is

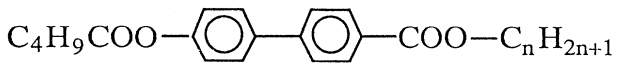

This group of molecules represents a relatively small modification (a change from alkoxy to acyloxy) to the *nm*OBC structure, which is rich in Hex-*B* behavior. Subsequent bulk heat-capacity results from 34COOBC and 64COOBC display weakly first-order Sm-*A*–Hex-*B* transitions [18].

Employing our high-resolution free-standing film calorimeter [6,7,] and electron-diffraction facility [19], we have carried out both thermal and structural investigations on free-standing films of 54COOBC. This compound exhibits the following bulk transition sequence [17]:

$$\text{isotropic} \xrightarrow[70\,^\circ\text{C}]{} \text{Sm-}A \xrightarrow[55\,^\circ\text{C}]{} \text{Hex-}B \xrightarrow[53\,^\circ\text{C}]{} \text{Cry-}B\ .$$

The existence of the Cry-*B* phase below the Hex-*B* phase differs from the typical *nm*OBC sequence in that the Hex-*B* phase is generally followed by the Cry-*E* phase in the *nm*OBC compounds. Besides extensive investigations

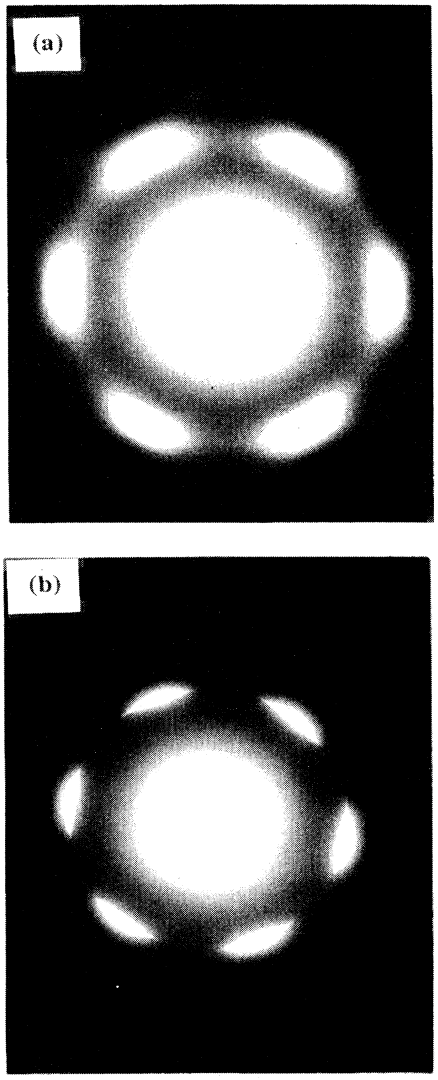

FIG. 2. Electron-diffraction pattern from (a) an eight-layer 3(10)OBC film and (b) a nine-layer 54COOBC film. The plates were purposely overexposed to check the existence of 12 weak herringbone diffraction spots in (a), but not in (b).

of the intriguing Sm-A–Hex-B transition, we have also probed the nature of the isotropic–Sm-A and Hex-B–Cry-B transitions in free-standing films. An unusual thinning transition above the bulk isotropic–Sm-A transition temperature has been found.

II. THE Sm-A–Hex-B–Cry-B TRANSITIONS

A. Experimental results

Detailed electron-diffraction investigations have been carried out to ensure that the Hex-B phase of 54COOBC possesses bond-orientational order but not herringbone order. Under the guidance of our calorimetric results, nine-layer 54COOBC films were studied over a wide temperature range covering the Sm-A, Hex-B, and Cry-B phases. As expected, the Sm-A phase yields a diffuse ring of constant intensity [see Fig. 3(a)]. The Hex-B phase displays one set of characteristic sixfold diffraction arcs [see Fig. 3(b)]. The exposure time is about 6 s with an electron-beam current density of about 0.1 electron/Å^2 s. Evidence for the existence of herringbone order in these Hex-B films can be obtained by increasing the exposure time to about 1 min and looking for satellite spots at a radial distance 32% beyond that of the hexatic arcs [5]. When this procedure was applied to the 3(10)OBC thin films, 12 satellite spots, indicative of herringbone order in three possible orientations, were discernible [see Fig. 2(a)]. In contrast, no herringbone spots are discernible in the overexposed diffraction pattern from 54COOBC Hex-B thin films in this study [see Fig. 2(b)], suggesting that the herringbone order is either not present or significantly weaker than that in nmOBC compounds. Thus, within our resolution, only the development of bond-orientational order is observed through the Sm-A–Hex-B transition of 54COOBC.

Upon further cooling, the films make a transition into the hexagonal Cry-B phase, featured by one set of six sharp diffraction peaks [see Fig. 3(c)]. This diffraction pattern is typical of another Cry-B material, namely N-(4-n-butyloxybenzylidene)-4-n-octylaniline (4O.8). The sharpness of the six diffraction peaks clearly indicates that the entire film is in the Cry-B phase. This is in contrast to the coexistence of the sharp peaks and hexatic arcs found in some temperature range of the 75OBC compound [20]. Because the higher (Sm-A) and lower (Cry-B) temperature phases clearly do not possess herringbone order in 54COOBC, it is extremely unlikely that the transition into the intermediate (Hex-B) phase would involve the formation of herringbone order only to be removed by the subsequent transition into the Cry-B phase. It is therefore reasonable to assume that, consistent with our electron-beam diffraction results, the Hex-B phase of 54COOBC does not exhibit herringbone order.

Employing our free-standing film calorimeter, we have measured the temperature variation of heat capacity (all films) and optical reflectivity (thin films only) for various 54COOBC film thicknesses. Figure 4 displays the heat-

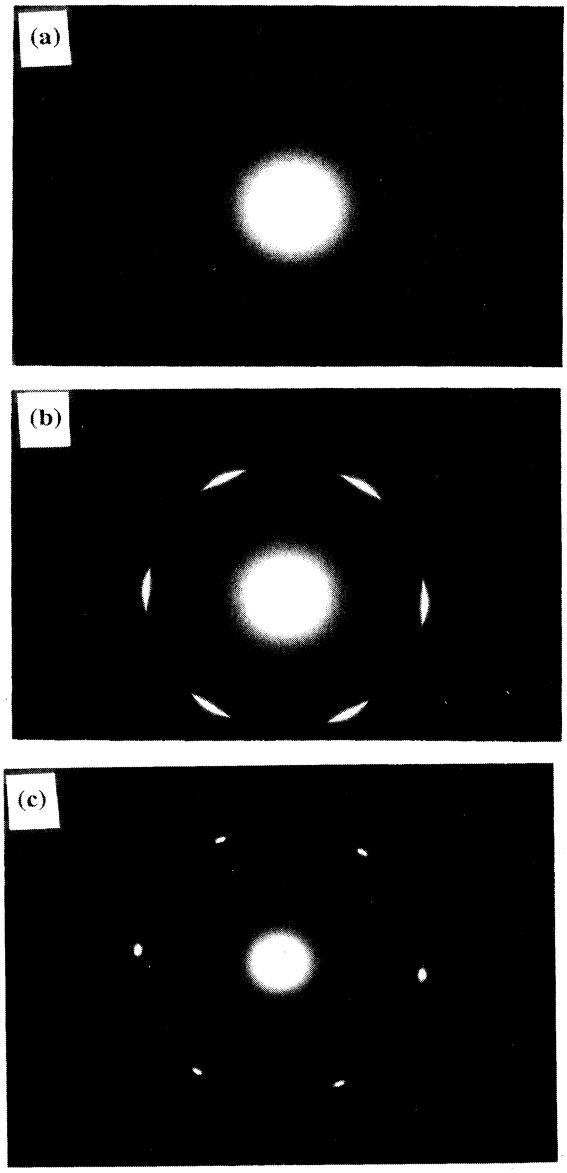

FIG. 3. Electron-diffraction patterns from a nine-layer 54COOBC film (a) in the Sm-A phase, (b) in the Hex-B phase, and (c) in the Cry-B phase.

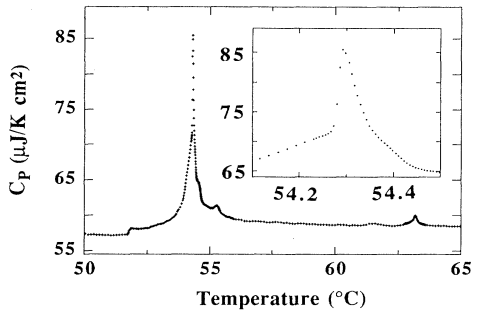

FIG. 4. Temperature dependence of heat capacity from a 100-layer 54COOBC film. The inset shows greater detail near the major heat-capacity peak.

capacity data from a 100-layer film. Above the main heat-capacity peak, three separate heat-capacity anomalies at around 54.5 °C, 55.5 °C, and 63.5 °C are clearly discernible. Based on previous x-ray and heat-capacity results of other liquid-crystal compounds, it is apparent that this series of transitions is due to layer-by-layer surface-enhanced transitions associated with the hexatic order. The anomaly near 63.5 °C can be attributed to the formation of hexatic order at two outermost layers. Below the main heat-capacity peak, a heat-capacity step near 52 °C is due to the Cry-*B* ordering. Upon cooling to approximately 44 °C, no additional heat-capacity anomaly was observed. Thus we do not know the extent of the Cry-*B* order (two outermost layers, the entire film, or something in between) in the temperature region below the observed heat-capacity step.

Three salient differences between the Sm-*A*–Hex-*B* and Hex-*B*–Cry-*B* transitions emerge. First of all, the former displays a layer-by-layer transition sequence and the latter shows only one transition. Second, the surface hexatic order exhibits a pronounced pretransitional heat-capacity contribution, but the Cry-*B* order displays only a sharp step in heat capacity. Third, while the surface hexatic order appears as a sharp peak down to the two-layer film, the step associated with the Cry-*B* order cannot be resolved for films thinner than seven layers.

The inset of Fig. 4 shows the heat capacity in the immediate vicinity of the main peak. The breaks in the slope of the heat capacity just above and below the peak temperature indicate that the transition is first order. We attribute these breaks (width approximately equal to 90 mK) to a narrow two-phase region that is likely due to a small amount of residual impurities or to structural defects. Similar magnitudes of two-phase regions have been reported in the heat-capacity data of bulk 34COOBC and 64COOBC near the Sm-*A*–Hex-*B* transition [18].

Both heat capacity and optical reflectivity obtained from a simultaneous measurement near the Sm-*A*–Hex-*B* transition of a two-layer film are displayed in Fig. 5. Similar to the case of 3(10)OBC [8], the heat capacity shows a single sharp symmetric peak while the optical reflectivity exhibits a smooth variation with a sign change in curvature near the peak position of the heat capacity. For unknown reasons, both heat-capacity and optical reflectivity data consistently display more scattering than those near the Sm-*A*–Hex-*B* transition of two-layer 3(10)OBC films. In the case of 3(10)OBC films, it has been established that optical reflectivity (R) is proportional to the integral of heat-capacity data. Thus R is directly related to the entropy change through the transition region. Assuming that this also holds for two-layer 54COOBC films, the absence of an observable step in optical reflectivity near the heat-capacity peak position suggests that, to within the scattering of our experimental data, there exists no additional δ-function-like latent heat.

Under several reasonable assumptions, the optical reflectivity (R) data can be directly related to the in-plane molecular density [8]. The result presented in Fig. 5 reflects the increase of in-plane molecular density as the temperature decreases. Over a temperature window T_1 $(=T_c-0.75\ \text{K}) < T < T_2$ $(=T_c+0.75\ \text{K})$, the relative optical reflectivity change $(\delta R=[R(T_1)-R(T_2)]/R(T_c))$ is about 4.8×10^{-3} for 54COOBC and 1.8×10^{-2} for 3(10)OBC. This comparison indicates that the 3(10)OBC compound experiences a larger increase in the in-plane molecular density through the Sm-*A*–Hex-*B* transition and favors some degree of herringbone orientational order.

Although the molecular structure of 54COOBC is very similar to that of *nm*OBC compounds, for unknown reasons, the former is much more susceptible to deterioration. Consequently, every 4 days we had to thoroughly clean the film plate and load a new sample into our calorimeter. Furthermore, the signal-to-noise ratios of the heat-capacity and optical reflectivity data on 54COOBC are consistently worse than those on the *nm*OBC compounds. These two factors lead to a much larger uncertainty in our thermal hysteresis measurements between successive heating and cooling runs. With a temperature ramping rate of about 10 mK/min near the heat-capacity peaks, detailed thermal hysteresis studies have been conducted. The hysteresis is found to be 80±50 mK. After adjusting the changes in transition temperatures between the successive cooling and heating runs, the shapes of the heat-capacity anomalies are approximately the same within our data scattering (see Fig. 6). Thus the two-layer 54COOBC film exhibits a weakly first-order Sm-*A*–Hex-*B* transition. In several experi-

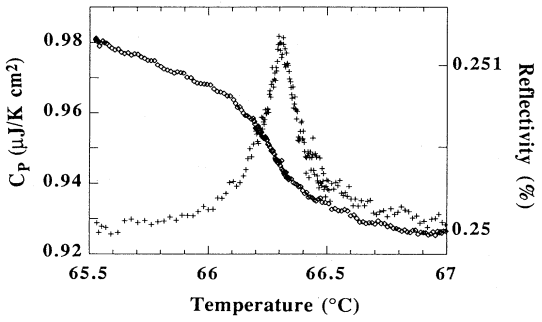

FIG. 5. Temperature variation of heat capacity and optical reflectivity near the Sm-*A*–Hex-*B* transition obtained from a simultaneous measurement of a two-layer 54COOBC film.

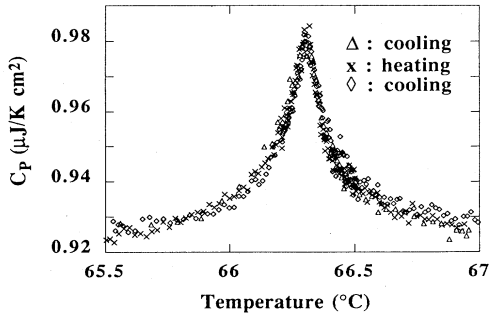

FIG. 6. Overlay of the successive cooling (△), heating (×), and cooling (◇) hysteresis runs from a two-layer 54COOBC film.

mental runs, we cooled the two-layer films down and did not detect any thermal signal associated with the Hex-B–Cry-B transition. At this moment, we do not know if this negative result is due to the fact that thermal signal associated with this transition is too weak to be resolved or there exists no such a transition in the two-layer film.

Heat-capacity data from three-, four-, six-, and nine-layer films are shown in Figs. 7 and 8. The experimental data are somewhat noisy. Similar to the cases found in nmOBC compounds, the heat-capacity peak from the single interior layer of a three-layer film is again more than a factor of 2 smaller than that of the four-layer film. Three well-separated and sharp heat-capacity peaks can be seen in the nine- and six-layer films. These clearly demonstrate the existence of surface induced layer-by-layer transitions.

Figure 9 shows an electron-diffraction pattern from a four-layer film at a temperature between the two heat-capacity peaks. The photograph, which is slightly overexposed in order to reveal the constant intensity ring, clearly displays the coexistence of a weak diffuse ring (from two interior Sm-A layers) and a set of sixfold arcs (from two surface Hex-B layers). The existence of one single set of the sixfold arcs indicates that the bond-orientational order existing on the two outermost surface layers is correlated with each other.

For the six-layer film, we have again measured thermal hysteresis of 30, 160, and 200 mK (with resolution of 50 mK) for the transitions associated with the surface, next-to-the surface, and interior layers, respectively. Moreover, the magnitudes of the heat-capacity peak heights differ by less than 5% between the heating and cooling runs. Thus the surface-layer transition of the six-layer film is seemingly continuous to within our resolution. The quasiadiabatic nature of our calorimeter prevents the detection of δ-function-type latent heat associated with first-order transitions. Consequently, it is not clear why the magnitude of the heat-capacity peak from the two outermost layers increases with the film thickness. This is different from that of nmOBC in which the magnitude of the surface heat-capacity anomaly remains the same as the film thickness varies [7].

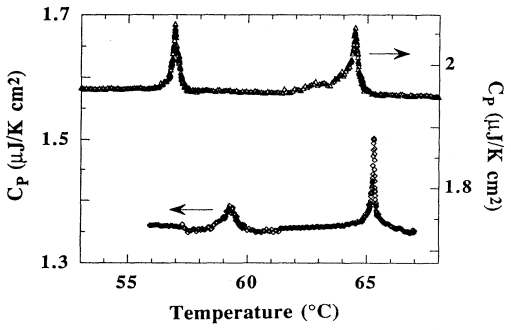

FIG. 7. Temperature dependence of heat capacity obtained from a three- (○) and four- (△) layer 54COOBC films near the Sm-A–Hex-B transition.

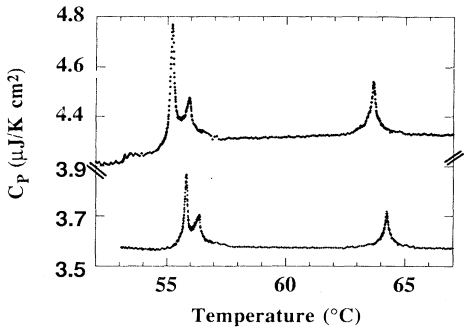

FIG. 8. Heat capacity versus temperature obtained from six- (+) and nine- (◇) layer 54COOBC films near the Sm-A–Hex-B transition.

The heat-capacity step associated with the Hex-B–Cry-B transition is still observable in the nine-layer film data but not in the films thinner than seven layers. Electron-diffraction results suggest that, in the Hex-B phase, these thinner films break upon cooling before transforming to the Cry-B phase.

B. Data analyses and discussions

The fact that the two-layer film exhibits a single heat-capacity anomaly indicates that it possesses two-dimensional thermal behavior. Although the transition is weakly first order, the pronounced pretransitional heat capacity and divergent character are in sharp contrast to the theoretical prediction (see Fig. 1). Two-dimensional melting theory suggests that the liquid-hexatic transition

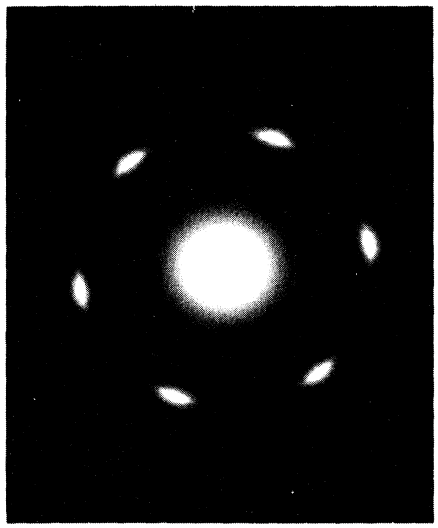

FIG. 9. Electron-diffraction pattern from a four-layer 54COOBC film. The data were taken in the temperature region between the two heat-capacity peaks shown in Fig. 7. The coexistence of the constant intensity ring (from the two interior layers in the Sm-A phase) and a set of sixfold arcs (from the two surface layers in the Hex-B phase) is clearly discernible.

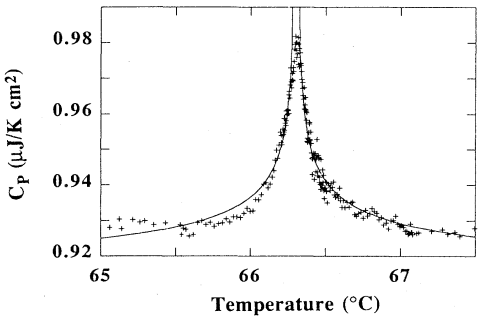

FIG. 10. Results from a simple power-law fitting to Eq. (1) (solid lines) of the two-layer film data yields a positive critical exponent α. Clearly, the experimental data are well characterized by this divergent heat-capacity expression, which is inconsistent with the theoretical prediction for the KT-type transition (see Fig. 1).

should exhibit a KT-type transition, with only an essential singularity, but no fluctuationlike heat-capacity contribution at the transition temperature [11]. The fittings of the heat-capacity anomalies of the two-layer film and the surface transition of the six-layer film (see Fig. 10) to a simple power law [Eq. (1)] yield $\alpha=0.30\pm0.07$ [21]. Due to the weakly first-order nature of this transition, the fitting window covers only approximately $1\frac{1}{2}$ decades in reduced temperature. Consequently, the existence of the herringbone order in the Hex-*B* phase of *nm*OBC compounds may not be the major source of the discrepancy between the two-dimensional melting theory and our experimental results. Based on these experimental observations, one might wonder if there is a hidden order parameter with a three-state Potts symmetry associated with the Sm-*A*–Hex-*B* transition of liquid crystals.

Similar to the 100-layer film data (see Fig. 4), the heat-capacity data from a 30-layer film also show three additional surface enhanced layer-by-layer transition peaks above the main one. Although we cannot experimentally determine whether the wetting transition is a complete or an incomplete one, the sequence of the transition temperatures $[T_c(L)]$ can be described by the simple power law

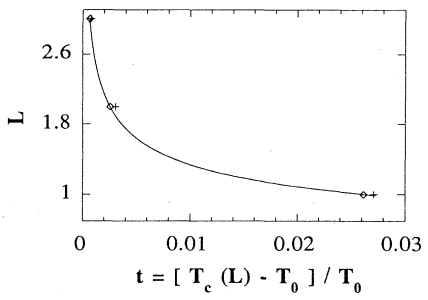

FIG. 11. L versus $[T_c(L)-T_0]/T_0$ and fitting curves from the surface-enhanced layer-by-layer transition sequence obtained from 100-layer (+) and 30-layer (◇) 54COOBC films.

$$L=L_0\{[T_c(L)-T_0]/T_0\}^{-\nu}. \quad (2)$$

Here L gives the separation (measured in units of layers) between the nearest film-vapor interface and the layer in question. The fitting yields $L_0=0.34\pm0.05$ (measured in units of layers) and the exponent $\nu=0.30\pm0.05$ and the results are shown in Fig. 11. Similar values of the exponent ν have been reported in the surface enhanced transitions near the Sm-*A*–Sm-*I* [22], Sm-*A*–Hex-*B* [23], and Sm-*A*–Cry-*B* transitions [24]. They all give $\nu=\frac{1}{3}$, characteristic of a van der Waals–like interlayer interaction [25].

III. THINNING TRANSITION ABOVE THE BULK SMECTIC-*A*–ISOTROPIC TRANSITION

The layer structure existing in the smectic phases makes the formation of free-standing liquid-crystal films possible. So far we have prepared and investigated free-standing films from more than 15 liquid-crystal compounds. Upon heating above the bulk Sm-*A*–nematic or Sm-*A*–isotropic transition temperature, all compounds except two rupture due to the lack of a layer structure in both the nematic and isotropic phases. First we discovered the remarkable layer-by-layer thinning transition above the Sm-*A*–isotropic transition of a partially perfluorinated compound, namely, H10F5MOPP (5-*n*-decyl-2-[4-*n*-(perfluoropentyl-metheleneoxy) phenyl] pyrimidine) [26]. Upon heating above the bulk Sm-*A*–isotropic transition temperature (T_{AI}), H10F5MOPP films first display an irregular thinning transition. Once the film thins down to nine molecular layers, it exhibits a regular layer-by-layer thinning transition down to two layers before rupturing at a temperature about 27 K above T_{AI}. This layer-by-layer thinning transition can be well characterized by a simple power law with exponent $\phi=0.74\pm0.02$.

Originally, we thought it to be a unique property of the perfluorinated compounds. To our surprise, similar thinning transitions have been found in 54COOBC above its bulk Sm-*A*–isotropic transition temperature. Although this layer thinning transition is not as regular as that of H10F5MOPP, one of the better runs is shown in Figs. 12 and 13. Upon heating an 11-layer film, we obtained a series of thinning transitions into nine-, eight-, five-, four-, three-, and two-layer films before it ruptured at a temperature about 10 K above the bulk T_{AI} ($\approx$70 °C). The film thickness can be determined from heat capacity (Fig. 12) or optical reflectivity data (Fig. 13). The inset of Fig. 12 exhibits a linear relation between the heat-capacity signal and layer thickness (N). Meanwhile, the inset of Fig. 13 shows another linear relation between the square root of optical reflectivity ($R^{1/2}$) and later number (N). In the H10F5MOPP compound, once the films had thinned to nine molecular layers, the transitions progressed basically in a layer-by-layer fashion. Here we have seen many irregularities. For example, before the films rupture, we have seen following sequences: 12, 4, and 3; 8, 5, and 4; etc. The data shown in Figs. 12 and 13 also exhibit some irregularities, namely, the eight-layer film existed over a much wider temperature range than

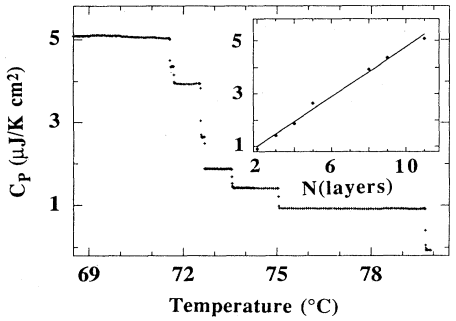

FIG. 12. Heat-capacity signal as a function of temperature above the bulk Sm-A–isotropic transition temperature (70 °C). Initially it was an 11-layer film; the film underwent a series of layer thinning transitions. The two-layer film remained stable over a 5 K temperature range before rupture at a temperature about 10 K above the bulk Sm-A–isotropic transition temperature. The inset displays a linear relation between the heat-capacity signal and layer thickness (N).

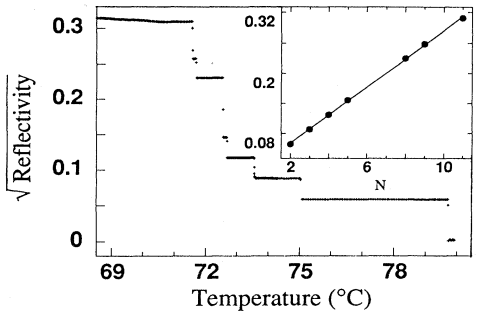

FIG. 13. Square root of optical reflectivity (normalized by incident laser beam intensity) versus temperature. The data were obtained from a simultaneous measurement with the heat capacity (shown in Fig. 12). The data also show a series of layer-thinning transitions. The inset displays a linear relation between the square root of the optical reflectivity signal and layer thickness (N).

both nine- and five-layer films. Nevertheless, the data can be described by a simple power law with exponent ($\phi=0.52$). Due to the irregularity in the thinning transition sequences found in 54COOBC, it is difficult to draw a strong conclusion on this exponent. The extremely sharp steps (less than 10 mK in width) and perfectly correlated between the two probes are the common features of the layer-thinning transition found above the Sm-A–isotropic transition of 54COOBC and H10F5MOPP. It would be interesting to investigate this unique layer-thinning transition in other liquid-crystal compounds [27] to see what kind of the unique physical properties prevent the smectic structure from rupturing just above the Sm-A–isotropic transition.

IV. CONCLUSION

The remarkable concept of bond-orientational order, proposed in the context of the two-dimensional melting theory, has been found to be extremely useful in describing numerous physical phenomena in condensed matter. To the best of our knowledge, only liquid crystals can provide a unique opportunity to check not only the structural but also thermal predictions of this model. The interpretation of the unexpected critical anomaly previously seen in the heat capacity near the Sm-A–Hex-B transition in two-dimensional nmOBC films and the surface transitions of thicker films has been complicated by the occurrence of herringbone order in addition to bond-orientational order in these materials. In this study, we have shown that, even in a compound such as 54COOBC for which careful electron-diffraction analysis indicates the absence of herringbone order, the inexplicable pretransitional divergence in the heat capacity is still present in thin films. The results indicate that the two-dimensional melting theory in its present form does not describe the remarkable liquid-hexatic transition in liquid-crystal thin films.

Similar to the other compounds, a surface-enhanced layer-by-layer transition near the Sm-A–Hex-B transition can be characterized by a simple power law with exponent $\upsilon=0.30$, indicative of the van der Waals interlayer interaction. Moreover, an unexpected layer-thinning transition has been found above the Sm-A–isotropic transition.

It would be ideal to identify or synthesize a liquid-crystal compound displaying a continuous Sm-A–Hex-B transition without herringbone order and then to conduct detailed thermal and structural investigations. Nevertheless, we will continue to study the unexpected layer-thinning transition occurring above the Sm-A–isotropic or Sm-A–nematic bulk transition temperature.

ACKNOWLEDGMENTS

This work was supported in part by the Supercomputer Institute, the University of Minnesota, and the National Science Foundation, Solid State Chemistry Program, Grant Nos. DMR-93-00781 and 91-03921. One of us (M.V.) would like to acknowledge support from the Department of Education.

*Author to whom correspondence should be addressed. Electronic address: huang001@maroon.tc.umn.edu

[1] J. M. Kosterlitz and D. J. Thouless, J. Phys. C **6**, 1181 (1973).

[2] B. I. Halperin and D. R. Nelson, Phys. Rev. Lett. **41**, 121 (1978); D. R. Nelson and B. I. Halperin, Phys. Rev. B **19**, 2457 (1979).

[3] A. P. Young, Phys. Rev. B **19**, 1855 (1979).

[4] C. C. Huang and T. Stoebe, Adv. Phys. **42**, 343 (1993), and references cited therein.
[5] R. Pindak, D. E. Moncton, S. C. Davey, and J. W. Goodby, Phys. Rev. Lett. **46**, 1135 (1981).
[6] R. Geer, T. Stoebe, T. Pitchford, and C. C. Huang, Rev. Sci. Instrum. **62**, 415 (1991).
[7] R. Geer, T. Stoebe, and C. C. Huang, Phys. Rev. E **48**, 408 (1993).
[8] T. Stoebe, C. C. Huang, and J. W. Goodby, Phys. Rev. Lett. **68**, 2944 (1992).
[9] T. Stoebe, I. M. Jiang, S. N. Huang, A. J. Jin, and C. C. Huang, Physica A **205**, 108 (1994).
[10] A. N. Berker and D. R. Nelson, Phys. Rev. B **19**, 2488 (1979).
[11] S. A. Solla and E. K. Reidel, Phys. Rev. B **23**, 6008 (1981).
[12] R. Bruinsma and G. Aeppli, Phys. Rev. Lett. **48**, 1625 (1982).
[13] I. M. Jiang, S. N. Huang, J. Y. Ko, T. Stoebe, A. J. Jin, and C. C. Huang, Phys. Rev. E **48**, 3240 (1993).
[14] G. Albertini, S. Melone, G. Poeti, F. Rustichelli, and G. Torquati, Mol. Cryst. Liq. Cryst. **104**, 121 (1984).
[15] C. C. Huang, G. Nounesis, and D. Guillon, Phys. Rev. A **33**, 2602 (1986).
[16] E. Gorecka, L. Chen, W. Pyzuk, A. Krowczynski, and S. Kumar, Phys. Rev. E **50**, 2863 (1994); G. Iannacchione, E. Gorecka, W. Pyzuk, S. Kumar, and D. Finotello, *ibid.* **51**, 3346 (1995).
[17] V. Surendranath, D. Fishel, A. de Vries, R. Mahmood, and D. L. Johnson, Mol. Cryst. Liq. Cryst. **131**, 1 (1985).
[18] R. Mahmood, M. Lewis, D. Johnson, and V. Surendranath, Phys. Rev. A **38**, 4299 (1988).
[19] M. Cheng, J. T. Ho, S. W. Hui, and R. Pindak, Phys. Rev. Lett. **59**, 1112 (1987).
[20] R. Geer, T. Stoebe, C. C. Huang, R. Pindak, G. Srajer, J. W. Goodby, M. Cheng, J. T. Ho, and S. W. Hui, Phys. Rev. Lett. **66**, 1322 (1991).
[21] A. J. Jin, M. Veum, T. Stoebe, C. F. Chou, J. T. Ho, S. W. Hui, V. Surendranath, and C. C. Huang, Phys. Rev. Lett. **74**, 4863 (1995).
[22] B. D. Swanson, H. Stragier, D. J. Tweet, and L. B. Sorensen, Phys. Rev. Lett. **62**, 909 (1989).
[23] T. Stoebe, R. Geer, C. C. Huang, and J. W. Goodby, Phys. Rev. Lett. **69**, 2090 (1992).
[24] A. J. Jin, T. Stoebe, and C. C. Huang, Phys. Rev. E **49**, R4791 (1994).
[25] J. G. Dash, in *Proceedings of the Nineteenth Solvay Conference,* edited by F. W. Dewitte (Springer-Verlag, New York, 1988).
[26] T. Stoebe, P. Mach, and C. C. Huang, Phys. Rev. Lett. **73**, 1384 (1994).
[27] Similar layer thinning transitions have been confirmed in other liquid crystal compounds. E. I. Demikhov, V. K. Dolganov, and K. P. Meletov, Phys. Rev. E **52**, 1285 (1995). Note : The reported layer-thinning transition near the Sm-A–nematic transition of 50.6 was observed in a very small opening [E. I. Demikhov (private communication)]. We have tried to repeat the same experiment even with an opening of 5 mm in diameter. The film always ruptured near the Sm-A–nematic transition temperature.

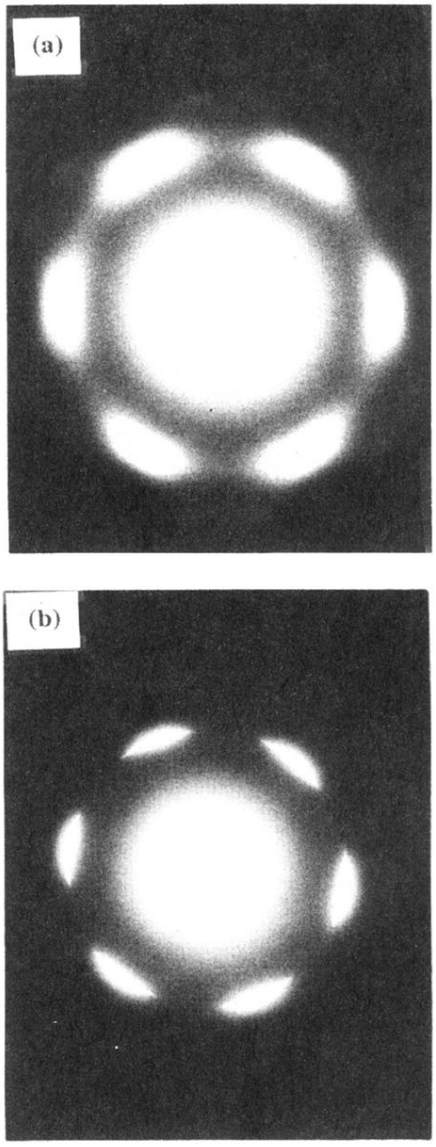

FIG. 2. Electron-diffraction pattern from (a) an eight-layer 3(10)OBC film and (b) a nine-layer 54COOBC film. The plates were purposely overexposed to check the existence of 12 weak herringbone diffraction spots in (a), but not in (b).

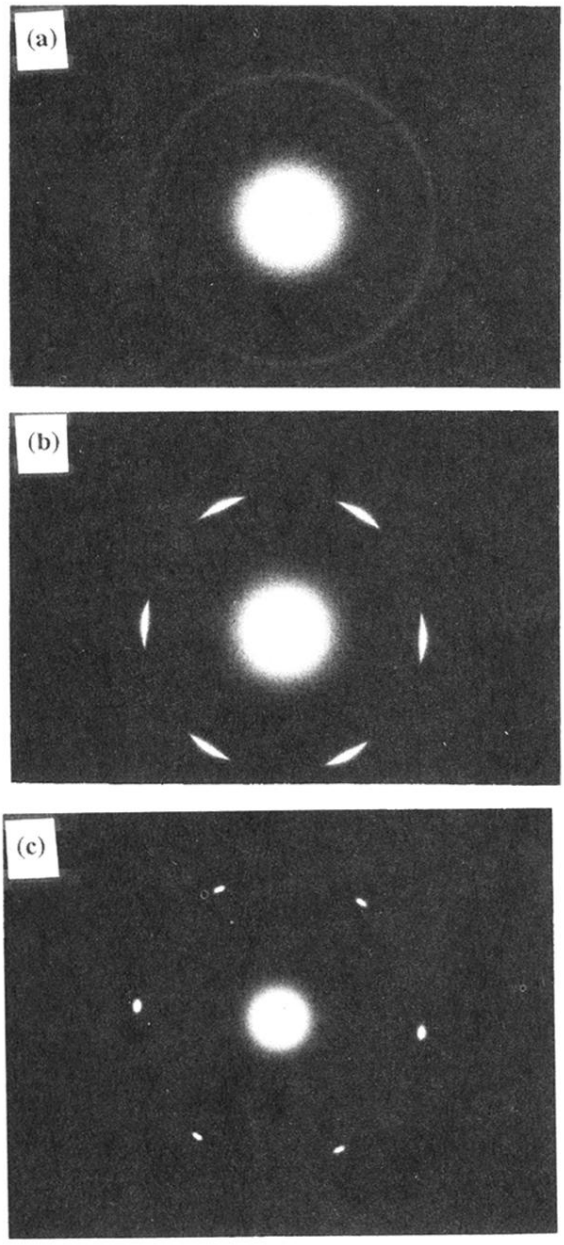

FIG. 3. Electron-diffraction patterns from a nine-layer 54COOBC film (a) in the Sm-*A* phase, (b) in the Hex-*B* phase, and (c) in the Cry-*B* phase.

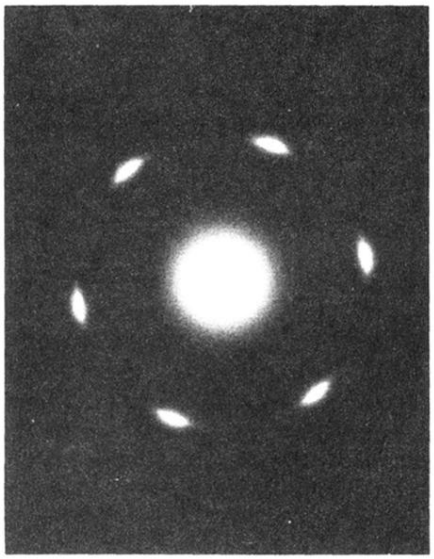

FIG. 9. Electron-diffraction pattern from a four-layer 54COOBC film. The data were taken in the temperature region between the two heat-capacity peaks shown in Fig. 7. The coexistence of the constant intensity ring (from the two interior layers in the Sm-*A* phase) and a set of sixfold arcs (from the two surface layers in the Hex-*B* phase) is clearly discernible.